

2
3 **Introduction**

4
5 Here we develop and analyse a baseline mathematical model of random ecDNA segregation
6 in exponentially growing tumour populations. This will allow us to work out a set of dynamic
7 predictions to distinguish ecDNA behaviour under neutral or positive selection. We will see
8 that certain properties, such as the mean ecDNA copy number per cell and the fraction of
9 cells with and without ecDNA fundamentally differ between these two scenarios.

10
11 We first present stochastic computer simulations using an agent-based model and compare
12 the simulations against experimental data. Next, we develop a complete and fine-grained
13 picture of ecDNA dynamics and work out the theoretical dynamics of moments as well as the
14 expected scaling of the ecDNA copy number distribution. This is followed by a simplified
15 deterministic approximation that will allow us to follow the change of cell populations with
16 and without ecDNA copies in time. These analytical results are compared both against
17 experimental data as well as stochastic simulations.

18
19 Our mathematical model is based on five assumptions: (i) ecDNA copies are segregated
20 randomly between daughter cells; (ii) the cell population is exponentially growing; (iii) ecDNA
21 replicates at the same rate as chromosomal DNA doubling during the cell cycle; (iv) the
22 population starts with a single cell carrying a single copy of ecDNA; (v) a cell that has lost all
23 ecDNA does not regain them.

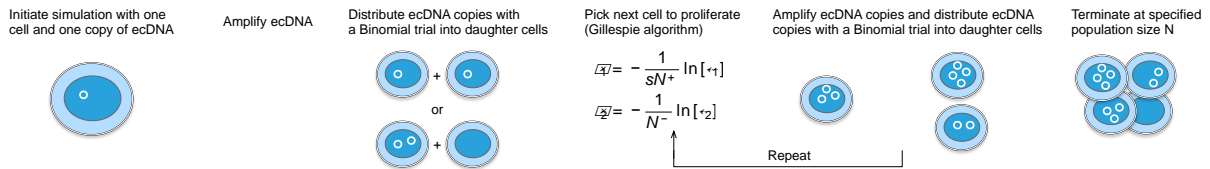
24
25 Our reasoning for these assumptions is as follows: (i) We have experimentally verified this
26 property across different cell lines with different ecDNA amplified genes. This is the
27 fundamental dynamic property that distinguishes ecDNA copy number evolution from the
28 evolution of somatic copy number alterations on chromosomes. (ii) We are interested in
29 ecDNA evolution in growing tumour populations. (iii) This assumption can be justified
30 retrospectively. If ecDNA is amplified with any coefficient > 2 the ecDNA copy number per
31 cell explodes within a few generations and each cell would be expected to carry thousands of
32 ecDNA copies. This ecDNA copy number inflation is not observed in any of the cell line or
33 patient data. (iv) Here we are interested in specific types of ecDNA amplifications. If we say a
34 cell carries k copies of ecDNA, we mean exactly k copies of one particular complex
35 amplification, e.g. EGFR in Glioblastoma or MYCN in Neuroblastoma. These are large and
36 complex genomic structures, and we assume that their origin is a single catastrophic event in
37 the evolutionary history of a tumour and a repeated production of the exact same circular
38 DNA structure containing millions of base pairs is extremely unlikely. There very well can be
39 situations, where cells carry multiple types (species) of ecDNA, e.g. an EGFR and MYC
40 amplification. In this situation, we would introduce two copy numbers k_1 and k_2 that keep
41 track of the temporal evolution of those two species independently. (v) ecDNA formation is a
42 rare, random event. Most ecDNA impose a metabolic load on the cell, are deleterious to its
43 fitness and lost rapidly. Very rarely, an ecDNA is created that carries a proliferative element
44 (e.g. an oncogene) which provides a growth and proliferative advantage to the cell.

45
46 Our notation will be as follows. $N(t)$ refers to the number of cells N at any particular time t
47 during the growth of the tumour. $N_k(t)$ refers to the number of cells with exactly k copies of

ecDNA at time t . The copy number per cell, k , can in principle range from zero to infinity. With this we can formulate the equation for the expected temporal change of cells with k ecDNA copies. For simplicity, we first explain the case of neutral ecDNA dynamics (cell with and without ecDNA have the same properties).

52
53
54
55

1.1 Agent based stochastic computer simulations of ecDNA segregation



56
57
58
59
60
61

Figure SI 1. Schematic of the stochastic simulations for random ecDNA segregation in exponentially growing tumour populations.

A schematic of the simulations can be found in Figure SI 1. All simulations are exact agent-based implementations of the underlying stochastic process. Simulations are initiated with a single cell carrying a single copy of ecDNA. Upon proliferation, the number of ecDNA copies in a cell are doubled and distributed between two daughter cells following a Binomial trial with success probability $1/2$. From thereon, the next cell to proliferate is chosen following a Gillespie algorithm. Briefly, we draw two random numbers ζ_1 and ζ_2 from a Uniform distribution in the interval $[0,1]$ and calculate the corresponding reaction times for cells with ecDNA (N^+) and cells without ecDNA (N^-), given by $\tau_1 = -\frac{1}{sN^+} \ln[\zeta_1]$ and $\tau_2 = -\frac{1}{N^-} \ln[\zeta_2]$. Whichever reaction time is smaller, is the next cell chosen for proliferation. Again, the ecDNA copy number of the cell is doubled and distributed into two daughter cells following a Binomial trial with success rate $1/2$. This process is iterated until the cell population reaches a predefined number of cells N . The same stochastic process can be used to simulate related dynamics for non-random ecDNA segregation. We just need to replace the Binomial trial by a segregation probability of interest, e.g. we could have non-random biased segregation with $p > 1/2$, or strict chromosomal segregation where each daughter cell always receives equal number of ecDNA copies. These simulations introduce two sources of stochasticity. The next cell to proliferate is picked at random, but proportional to fitness. The Gillespie algorithm (Gillespie, Journal of Physical Chemistry 1977) offers an exact stochastic implementation of the underlying Markov Chain and its implementation is standard in these types of individual based simulations. The second source of randomness emerges from the segregation of ecDNA copies into daughter cells after division. Computer simulations of (non)random ecDNA segregation have been implemented in C++ and the code to run the simulations is available <https://github.com/BenWernerScripts>.

85
86

1.2 Comparison of stochastic simulations and experimental observations

87
88
89
90

The final output of our stochastic simulations is a population of cells, each cell with a particular ecDNA copy number. These copy number distributions can be followed over time, and all information of interest, e.g. the population of cells with and without ecDNA, the mean

91 and variance of the ecDNA distribution, the actual ecDNA copy number distribution as well as
 92 the power law scaling of the ecDNA distribution can be constructed.

93

94 We use a Kolmogorov-Smirnov test to compare the ecDNA copy number distributions from
 95 stochastic computer simulations and experimentally observed distributions in patients or cell
 96 line experiments. The test first gives the KS_d distance, with smaller values indicating better
 97 agreement. It also allows us to calculate a p_{KS} value. The test compares two probability
 98 distributions for distance d , the p -value corresponds to the probability of obtaining d or
 99 smaller given the that the two distributions are different. For the ecDNA copy number
 100 distributions, we also use the Shapiro-Wilk statistics, to test for deviations from a normal
 101 distribution. In addition, to show goodness of fits, we added Quantile-Quantile plots for all
 102 comparisons of experimental and theoretical distributions.

103

Sample	KS_d^{random}	p_{KS}^{random}	$KS_d^{\text{non-random}}$	$p_{KS}^{\text{non-random}}$	$p_{\text{ShapiroWilk}}$	#samples
PC3_Myc	0.065	0.375	0.46	0	0.758	200
SNU16_Myc	0.039	0.918	0.49	0	0.939	194
SNU16_fgfr2	0.063	0.415	0.49	0	4.2×10^{-9}	196
GBM39_EGFR	0.072	0.221	0.46	0	0.001	210
COLO_Myc	0.033	0.973	1	0	0.196	206

104

105 **Table SI 1.** Test statistics to compare the theoretical distributions with experimental observations for the single
 106 cell ecDNA segregation probabilities as presented in Figure 1c in the main text. The similarity of the two
 107 distributions is tested by a Kolmogorov-Smirnov test for two competing hypothesis, random ecDNA segregation
 108 and non-random chromosomal segregation. We also test for normality using the Shapiro-Wilk statistics.

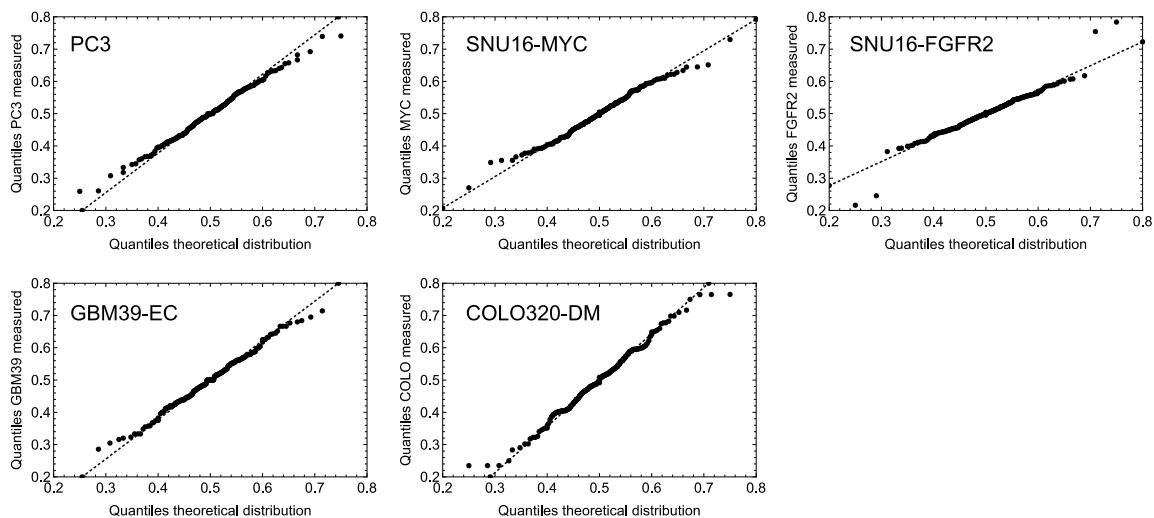
109

Sample	KS_d^{random}	p_{KS}^{random}	$KS_d^{\text{non-random}}$	$p_{KS}^{\text{non-random}}$	$p_{\text{ShapiroWilk}}$	#samples
PC3_Myc	0.091	0.074	0.986	0	3.1×10^{-13}	200
SNU16_Myc	0.052	0.662	0.999	0	9.9×10^{-4}	194
SNU16_fgfr2	0.066	0.359	1	0	1.9×10^{-12}	196
GBM39_EGFR	0.071	0.237	0.977	0	6.6×10^{-9}	210
COLO_Myc	0.075	0.196	0.994	0	2.4×10^{-11}	206
GBM1	0.141	0.073	0.882	0	0.019	85
GBM2	0.082	0.914	0.757	0	0.028	46
GBM3	0.138	0.131	0.843	0	0.003	72
GBM4	0.254	0.004	0.759	0	0.014	101
GBM5	0.163	0.01	0.831	0	0.004	103
GBM6	0.159	0.124	0.833	0	0.057	55
Chp212	0.193	0.048	0.963	0	1.2×10^{-10}	154
TR14_MYCN	0.047	0.681	0.987	0	1.6×10^{-8}	232
TR14_CDK4	0.091	0.174	0.855	0	1.7×10^{-13}	284
NB4	0.098	0.177	1	0	1.2×10^{-8}	126
NB7	0.129	0.313	0.999	0	4.8×10^{-3}	56
NB8	0.074	0.375	0.983	0	1.3×10^{-6}	151
NB10	0.176	0.004	0.996	0	3.3×10^{-6}	98
NB13	0.271	0.001	0.999	0	0.004	155

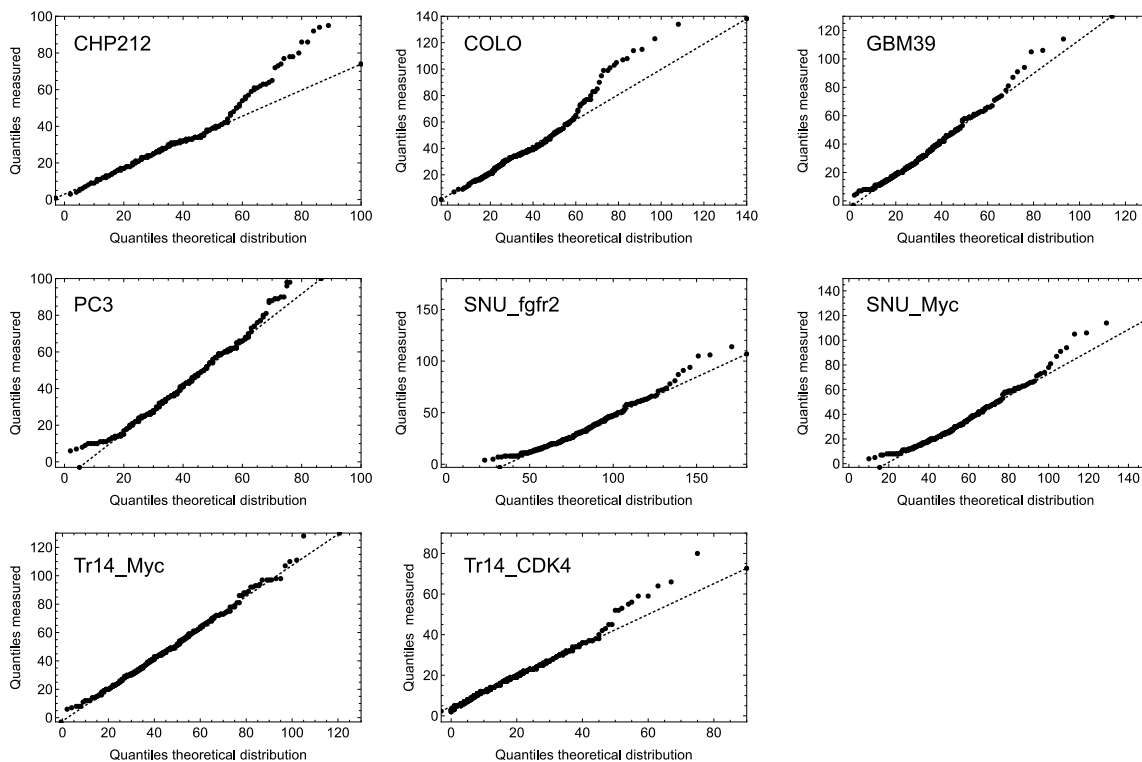
110

111 **Table SI 2.** Test statistics to compare the theoretical ecDNA copy number distributions with experimental
 112 measured ecDNA copy number distributions in patient and cell line data as presented in Figure 2 b and c in the
 113 main text. The similarity of the two distributions is tested by a Kolmogorov-Smirnov test for two competing

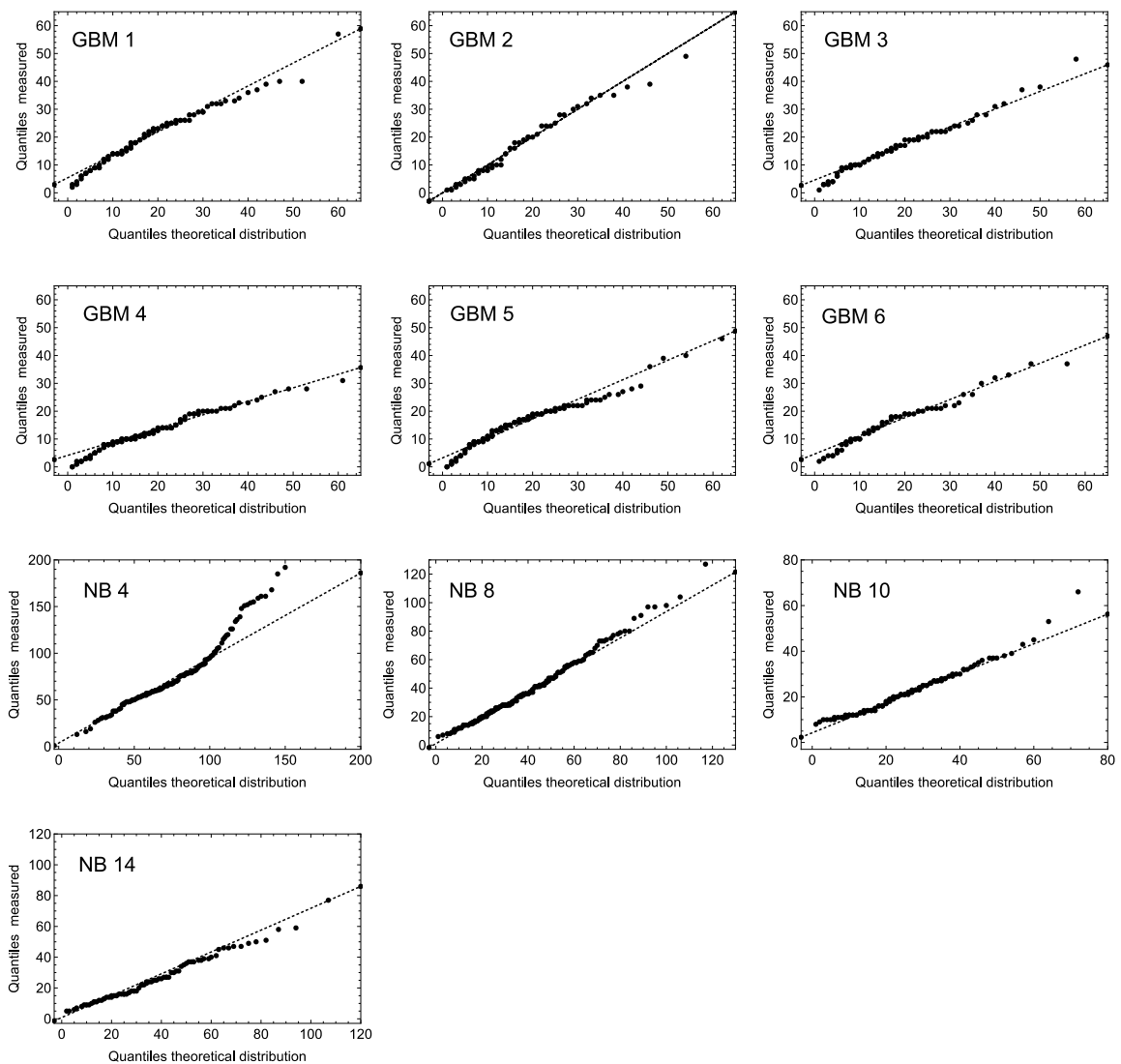
114 hypothesis, random ecDNA segregation and non-random chromosomal segregation. We also test for normality
 115 using the Shapiro-Wilk statistics.
 116
 117



118
 119 **Figure SI 2.** Quantile-Quantile_plots to compare the theoretical and experimental distributions from single
 120 cell ecDNA segregation probabilities presented in Figure 1c in the main text.
 121
 122
 123



124
 125 **Figure SI 3.** Quantile-Quantile_plots to compare the theoretical and experimental ecDNA copy number
 126 distribution in cell lines presented in Figure 2b in the main text.
 127
 128
 129
 130
 131

133
134

135 **Figure SI 4.** Quantile-Quantile_plots to compare the theoretical and experimental ecDNA copy number
 136 distribution in samples of Glioblastoma and Neuroblastoma patients presented in Figure 2c in the main text.

137

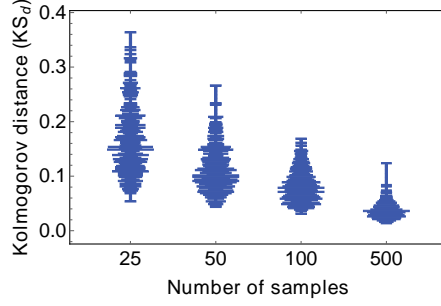
138

139

140 **1.3 Finite sampling and resolution limits**

141

142 In our stochastic simulations, we have the freedom to in principal sample and analyse as many
 143 single cell ecDNA copy number profiles as we want. This is obviously not the case in our
 144 experimental data due to technical and financial limitations. We thus tested if we can
 145 reconstruct the ecDNA copy number distribution with limited single cell resolutions. We
 146 generated a distribution of ecDNA copy numbers by simulating a tumour with 10^7 cells and
 147 ecDNA under positive selection $s = 2$. We then sampled 10,000 times 25, 50, 100 and 500
 148 cells respectively, constructed the ecDNA copy number distribution and calculated the
 149 Kolmogorov distance



150
151

152 **Figure SI 5.** Sampling of the ecDNA copy number distribution. We took 10^4 samples with 25, 50, 100 and 500
153 cells respectively from a single simulation of the ecDNA distribution of 10^7 cells. Shown are the corresponding
154 distributions of Kolmogorov distances. Resolution increases with sample size. Kolmogorov distances for samples
155 of 100 cells are comparable to our experimental observations.

156
157

158 of the sampled distribution to the true (non-sampled) distribution. As expected, the
159 resolution increases with sample size. More importantly, we find Kolmogorov distances that
160 are comparable to experimental data comparisons and a sample size in the order of 100 cells
161 already allows us to capture important aspects of the ecDNA copy number distribution.

162
163

164 2.1 Stochastic dynamics of ecDNA copy numbers under neutral selection

165
166
167

The dynamic equation for the number of cells $N_k(t)$ with k neutral copies of ecDNA with time t becomes

$$168 \quad \frac{dN_k(t)}{dt} = -N_k(t) + 2 \sum_{i=\lceil k/2 \rceil}^{\infty} N_i(t) \binom{2i}{k} \frac{1}{2^{2i}}$$

169

170 This is a set of, in principal, infinitely many coupled differential equations, formally known as
171 the Master equation of the underlying Markovian stochastic process. It describes the
172 evolution of all states the system at question can be in. In our case, all possible states
173 correspond to the number of cells with k copies of ecDNA. The left-hand side is the time
174 derivative of the number of cells with k ecDNA copies. The right-hand side collects all possible
175 events (rates) that change this number. If a cell with k copies divides, its copies are amplified
176 and randomly distributed between both daughter cells. This reduces the number of cells with
177 exactly k copies, reflected by the first term $-N_k(t)$. The second term on the right-hand side
178 of the equation collects all cells of the system that gain k copies of ecDNA due to random
179 segregation amongst daughter cells. Upon cell proliferation, $2i$ copies are randomly
180 segregated amongst two daughter cells. The number of ecDNA copies k in a daughter cell
181 follows a Binomial distribution with success rate $1/2$

182

$$183 \quad B\left(k \mid n = 2i, p = \frac{1}{2}\right) = \binom{2i}{k} \frac{1}{2^{2i}}$$

184

185 It turns out that working with cell densities ρ_k rather than total cell numbers N_k is
186 advantageous. We therefore decouple population growth and demographic changes and
187 write $N_k(t) = N(t)\rho_k(t)$ with $\sum_{i=1}^{\infty} \rho_i(t) = 1$ and $N(t) = \sum_k N_k(t)$ denotes the total

188 number of cells at time t . We first can check that the structure of our equations is correct and
 189 we recover an exponentially growing population for $N(t)$ as we have claimed in our initial
 190 assumptions. We can write:

191

$$\begin{aligned}
 \frac{dN(t)}{dt} &= -N(t) + 2N(t) \sum_{k=0}^{\infty} \sum_{i=\lceil k/2 \rceil}^{\infty} \rho_i(t) \binom{2i}{k} \frac{1}{2^{2i}} \\
 &= -N(t) + 2N(t) \sum_{i=0}^{\infty} \rho_i(t) \frac{1}{2^{2i}} \sum_{k=0}^{2i} \binom{2i}{k} \\
 &= -N(t) + 2N(t) \sum_{i=0}^{\infty} \rho_i(t) \frac{1}{2^{2i}} 2^{2i} = N(t)
 \end{aligned}$$

195

196 And we do find that the total population grows exponentially in time $N(t) = N(0)e^t$. This
 197 allows us to write for the temporal change of cell densities ρ_k with k ecDNA copy numbers:

198

$$\frac{d\rho_k(t)}{dt} = -2\rho_k(t) + 2 \sum_{i=\lceil k/2 \rceil}^{\infty} \rho_i(t) \binom{2i}{k} \frac{1}{2^{2i}}$$

200

201

202 **2.2 Dynamics of Moments of ecDNA copies under neutral selection**

203

204 The Master equations above describe the full dynamics of the probability densities of the
 205 ecDNA copy number distribution. They therefore encode in principle all properties of the
 206 underlying stochastic process. However, a complete analytical treatment is challenging.
 207 Nevertheless, many aspects of the system are analytically tractable. We first discuss the
 208 dynamics of the moments of the ecDNA copy number distribution. In particular we are
 209 interested in the first and second moment, as they are directly related to the mean ecDNA
 210 copy number per cell and the expected variance of the ecDNA copy number distribution.

211

212 With above equation for the density of cells with k ecDNA copies, we can calculate the
 213 moments of the underlying probability density function. In general, the l -th moment is
 214 calculated via

215

$$M^{(l)}(t) = \sum_{i=0}^{\infty} i^l \rho_i(t)$$

216

217 The moment $M^{(0)}(t)$ is just the sum over the density and by definition constant. The first
 218 moment corresponds to the average number of ecDNA copies per cell and we can write:

219

$$\begin{aligned}
 \frac{dM^{(1)}(t)}{dt} &= -2M^{(1)}(t) + \sum_{k=0}^{\infty} \sum_{i=\lceil k/2 \rceil}^{\infty} k \rho_i(t) \binom{2i}{k} \frac{1}{2^{2i}} \\
 &= -2M^{(1)}(t) + \sum_{i=0}^{\infty} \rho_i(t) \frac{1}{2^{2i}} \sum_{k=0}^{2i} k \binom{2i}{k}
 \end{aligned}$$

221

222
$$= -2M^{(1)}(t) + \sum_{i=0}^{\infty} \rho_i(t) \frac{1}{2^{2i}} (2i)2^{2i-1} = 0$$

223
224

225 We therefore find $M^{(1)}(t) = \text{const}$ and the constant is given by the initial conditions. In most
226 cases discussed here, we will have $M^{(1)}(t) = M^{(1)}(t = 0) = 1$. In the case of neutral ecDNA
227 dynamics starting from a single cell containing a single copy of ecDNA, on average the
228 population maintains one copy of ecDNA per cell.

229

230 Next, we are interested in the second moment $M^{(2)}(t)$. Following our calculations for the first
231 moment we can similarly write:

232

233
$$\frac{dM^{(2)}(t)}{dt} = -2M^{(2)}(t) + \sum_{k=0}^{\infty} \sum_{i=\lceil k/2 \rceil}^{\infty} k^2 \rho_i(t) \binom{2i}{k} \frac{1}{2^{2i}}$$

234
$$= -2M^{(2)}(t) + \sum_{i=0}^{\infty} \rho_i(t) \frac{1}{2^{2i}} \sum_{k=0}^{2i} k^2 \binom{2i}{k}$$

235
$$= -2M^{(2)}(t) + \sum_{i=0}^{\infty} \rho_i(t) \frac{1}{2^{2i}} (2i + (2i)^2)2^{2i-2} = M^{(1)}(t)$$

236

237 With the initial conditions for the mean ecDNA copy numbers above we find the expression
238 $M^{(2)}(t) = t + \text{const}$. The constant can be fixed by the realisation that the variance of the
239 ecDNA copy number distribution at time $t = 0$ should equal 0 and we get $\text{Var}(t = 0) =$
240 $\text{const} - 1^2 = 0$, and therefore $\text{const} = 1$ and simply have that the variance increases linearly
241 in time for neutral ecDNA copies, $\text{Var}(t) = t$.

242

243

244

245

246

247

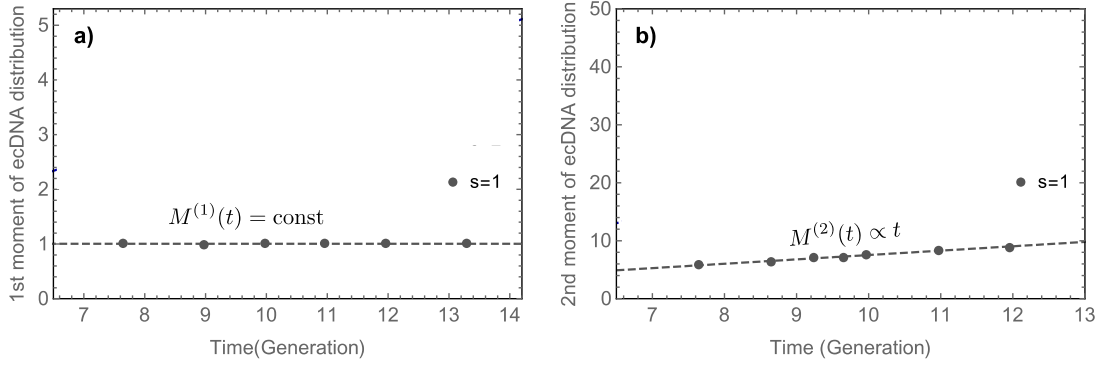
248

249

250

251

252



253
254
255
256
257

Figure SI 6. a) First and **b)** second moment of the ecDNA copy number distribution under neutral selection ($s = 1$). The mean number of ecDNA copies remains constant and the variance increases linearly in time. Stochastic simulations (points) are in very good agreement to theoretical predictions of polynomial increasing moments with time (dashed lines).

258
259

2.3 The scaling of the ecDNA copy number distribution in the continuous limit wave approximation

260
261
262
263
264
265
266
267

In the following, we are interested in the scaling behaviour of the ecDNA copy number distribution, e.g. what is the probability for a single cell to carry many copies of ecDNA. We will find that the right-hand tail of the ecDNA distribution towards large copy number scales with a power law inversely proportional to the copy number k .

268
269
270
271
272
273

Our general time dynamics describe discrete copy number states. To make further analytical progress, we now consider continuous states in the following calculations. This is an approximation that works well for the case of many ecDNA copies, but might be inaccurate for cells with very few copies of ecDNA. Under this continuous assumption, the change of the ecDNA copy number distribution becomes

274

$$\frac{d\rho_k(t)}{dt} = -2\rho(k, t) + \frac{2}{\sqrt{\pi}} \int_{k/2}^{\infty} dy \frac{\rho_y(t)}{\sqrt{y}} e^{\frac{(k-y)^2}{y}}$$

275
276
277
278

Where we replaced the Binomial with a Normal distribution. Given the exponential character of the ecDNA distribution, we proceed with an Ansatz in the form of a scaling wave solution

279
280

$$\rho_k(t) = e^{-vt} \Omega(ke^{-vt}).$$

281
282

Plugging our ansatz into the differential equation for the density ρ and setting $\frac{k}{2} \rightarrow 0$, we get

283

$$\frac{d}{dt} [e^{-vt} \Omega(ke^{-vt})] = -2e^{-vt} \Omega(ke^{-vt}) + \frac{2}{\sqrt{\pi}} \int_{k/2}^{\infty} dy \frac{e^{-vt} \Omega(ke^{-vt})}{\sqrt{y}} e^{\frac{(k-y)^2}{y}}$$

284
285
286

With $z = ke^{-vt}$ and $v = 2$, this transforms into

287

$$-z \frac{d}{dz} \Omega(z) = \frac{1}{\sqrt{\pi}} \int_{-\infty}^{\infty} dm \Omega(z) \frac{1}{\sqrt{z}} e^{\frac{-m^2}{z}} = \Omega(z).$$

288
289
290
291

This has the solution $\Omega(z) = c/z$ with an undetermined integration constant c . Plugging this back into our original ansatz and reversing all substitutions, this gives us for the scaling of the ecDNA copy number distribution

292
293

$$\rho_k(t) = \frac{c}{k}.$$

294
295
296
297
298
299

This predicts a power law scaling of the right-hand side tail of the ecDNA copy number distribution. Cells with very large copy number status become increasingly less likely for increasing k , for a sufficiently large tumour population, a considerable fraction of cells is expected to have large ecDNA copy number. This is indeed supported by observations both in cell line and patient data, where we recover these power law dependencies.

300
301

3.1 Stochastic dynamics of ecDNA copies under constant positive selection

302
303
304
305
306
307

In the previous sections, we discussed the stochastic dynamics of extra-chromosomal DNA under neutral selection. In that scenario, ecDNA is present in cells, but does not change the proliferative fitness of the cell. Next, we consider the case of ecDNA that is under positive selection, or in other words, ecDNA that gives a positive fitness advantage to cells. This will be of particular interest to the dynamics and diversification of ecDNA in cancerous tissues.

308
309
310
311
312

In order to model a selection advantage, we introduce a selection coefficient $s > 0$. In this notation, $s = 1$ corresponds to neutral dynamics, $s > 1$ to a selection advantage of cells with ecDNA and $0 \leq s < 1$ to a selection disadvantage of cells without ecDNA. The Master equation then needs to be modified in the following way

313
314
315

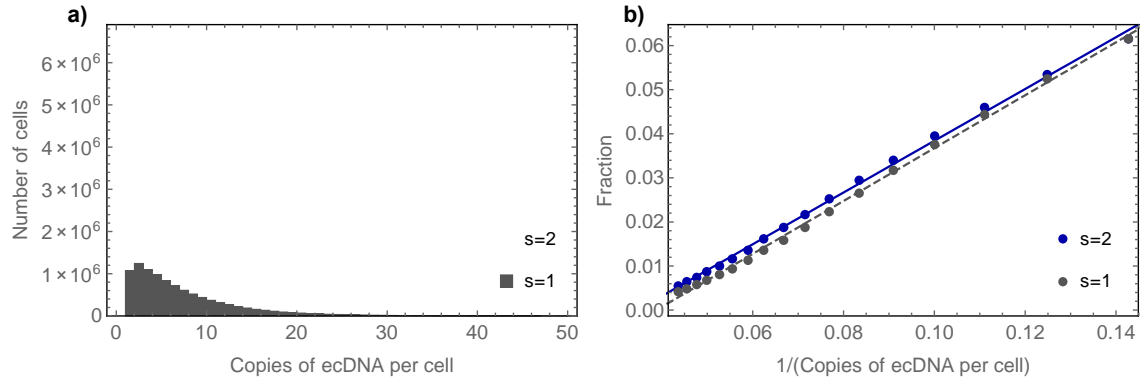
$$\begin{aligned} \frac{dN_k(t)}{dt} &= -sN_k(t) + 2s \sum_{i=\lceil k/2 \rceil}^{\infty} N_i(t) \binom{2i}{k} \frac{1}{2^{2i}} \\ \frac{dN_0(t)}{dt} &= N_0(t) + 2s \sum_{i=1}^{\infty} N_i(t) \frac{1}{2^{2i}} \end{aligned}$$

318
319

It can easily be checked that for $s \rightarrow 1$, we recover the Master equation in the neutral selection case. Above general Master equation for the selection case can also be written in a more compact form. Changing to the densities again, this compact form is given by

320
321
322
323
324
325
326

$$\begin{aligned} \left. \frac{d\rho_k(t)}{dt} \right|_{k>0} &= s \left. \frac{d\rho_k(t)}{dt} \right|_{s=1} + (s-1)\rho_k\rho_0 \\ \left. \frac{d\rho_0(t)}{dt} \right|_{s=1} &= s \left. \frac{d\rho_k(t)}{dt} \right|_{s=1} + (s-1)(1-\rho_0)\rho_0 \end{aligned}$$



327
 328 **Figure SI 7.** Distribution and scaling of the ecDNA copy number distribution. **a)** Distribution of the ecDNA copy
 329 number distribution for neutral (grey) and positively selected (blue) ecDNA evolution for 1000 repeats of
 330 stochastic simulations for tumours of 10^4 cells. Overall, more cells carry copies of ecDNA if positively selected
 331 compared to the neutral case. **b)** The scaling of the right-hand tail of the ecDNA distribution follows the predicted
 332 $1/k$ scaling (dots = stochastic simulations, lines = theoretical expectation).

333
 334

335 Allowing for selection adds an additional non-linear term to the original Master equation. We
 336 can also check the growth of the tumour population with ecDNA under positive selection. The
 337 equation for the total population now becomes

338

$$\frac{dN(t)}{dt} = sN(t) - (s - 1)\rho_0(t)N(t).$$

339

340 The second term on the right-hand side of the equation contains the density of cells without
 341 ecDNA $\rho_0(t)$. We do not have a general solution for this expression, but we will see later
 342 that $\rho_0(t \rightarrow \infty) \rightarrow 0$. Consequently, for sufficiently large N the tumour population will grow
 343 exponentially with $N_{s>1} = e^{st}$. Or, if we compare the relative change of fitness at any given
 344 time t we get

345

$$\text{Log}[N_{s>1}(t)] - \text{Log}[N_{s=1}(t)] = (s - 1)t.$$

346

347 In the initial phase of tumour growth, the term $-(s - 1)\rho_0(t)N(t)$ in above equation cannot
 348 be neglected and the growth will be in the interval

349

$$t \leq \text{Log}[N_{s>1}(t)] \leq st$$

350

351 slowly approaching the slope of st with increasing time.

352

353 **3.2 Dynamics of Moments of ecDNA copies under positive selection**

354

355 In the following we discuss the dynamics of Moments for ecDNA under positive selection.
 356 Following the steps above and using the generalised Master equation for the selection case,
 357 we find the following dynamic equation for the Moments

358

$$\frac{dM^{(l)}(t)}{dt} = s \frac{dM^{(l)}(t)}{dt} \Big|_{s=1} + (s - 1)\rho_0 M^{(l)}(t).$$

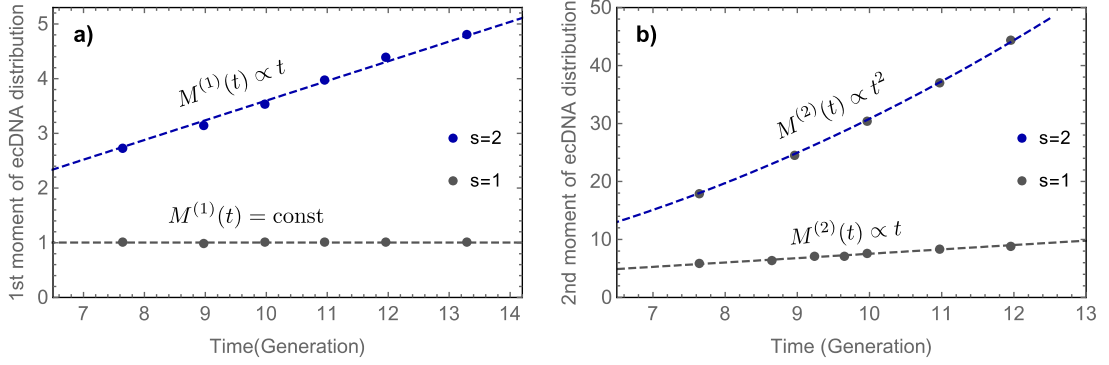
359

360

361

362

363



364
365

366 **Figure SI 8. a)** First and **b)** second moment of the ecDNA copy number distribution. In the neutral case ($s = 1$,
367 grey) the mean number of ecDNA copies remains constant and the variance increases linearly in time. Under
368 positive selection ($s = 2$, blue) the mean number of ecDNA copies increases in time. Stochastic simulations
369 (points) are in very good agreement to theoretical predictions of polynomial increasing moments with time
370 (dashed lines).

371
372

373 This implies for the first moment $\frac{dM^{(1)}(t)}{dt} = (s - 1)\rho_0 M^{(1)}(t)$, which then can be solved for
374 the first moment

375

$$376 M^{(1)}(t) = e^{(s-1)\int_0^t d\tau \rho_0(\tau)}.$$

377

378 Importantly, for positive selection we have $s > 1$ and therefore $s - 1 > 0$. Furthermore, the
379 integral is strictly positive, such that the first moment is expected to increase over time. In
380 other words, in a growing tumour population with ecDNA under positive selection, we expect
381 the average ecDNA copy number per cell to increase in time. This is in contrast to the neutral
382 case, where the average ecDNA copy number is expected to remain constant over time.

383

384 Similarly, the dynamic equation for the second moment becomes

$$385 \frac{dM^{(2)}(t)}{dt} = M^{(1)}(t) + (s - 1)\rho_0 M^{(2)}(t) \text{ and we find}$$

386

$$387 M^{(2)}(t) = tM^{(1)}(t).$$

388

389

390 The second moment is increasing as well, but now with an additional factor t compared to
391 the neutral case. Similar to the argument above, it follows that higher moments follow the
392 form

393

$$394 M^{(l)}(t) = P_l(t) e^{(s-1)\int_0^t d\tau \rho_0(\tau)} \sim t^{l-1} M^{(1)}(t).$$

395

396

397

398 **4.1 Deterministic population dynamics**

399

400 We have in the chapters above discussed stochastic aspects of the ecDNA copy number
 401 distribution for positive and neutral selection. Another question of interest is how the fraction
 402 of cells with and without ecDNA change in a growing tumour population. We therefore
 403 change the formulation of our mathematical model to a more coarse-grained picture and only
 404 consider cells with ecDNA $N^+(t)$ and cells without ecDNA $N^-(t)$. For cells with ecDNA, we
 405 do not distinguish between different copy number states. With the notation of the former
 406 chapters, we identify $N^-(t) = N_0(t)$ and $N^+(t) = \sum_{k=1}^{\infty} N_k(t)$.

407
 408 We can write for the change of these cells in time t

409
 410
$$\frac{dN^-(t)}{dt} = N^-(t) - v(N^+(t))N^+(t)$$

 411
$$\frac{dN^+(t)}{dt} = v(N^+(t))N^+(t)$$

412
 413 where $v(N^+(t))$ is the rate at which cells with ecDNA lose all ecDNA copies by chance due to
 414 complete asymmetric random ecDNA segregation (one daughter cell inherits all copies of
 415 ecDNA, while the other cell does not inherit any). Looking at the fraction of cells with ecDNA
 416 $f^-(t) = \frac{N^-(t)}{N^+(t) + N^-(t)}$, we can write

417
 418
$$\frac{d}{dt} \left(\frac{N^-(t)}{N^+(t) + N^-(t)} \right) = \frac{d}{dt} f^-(t) = (1 - f^-(t)) v(N^+(t))$$

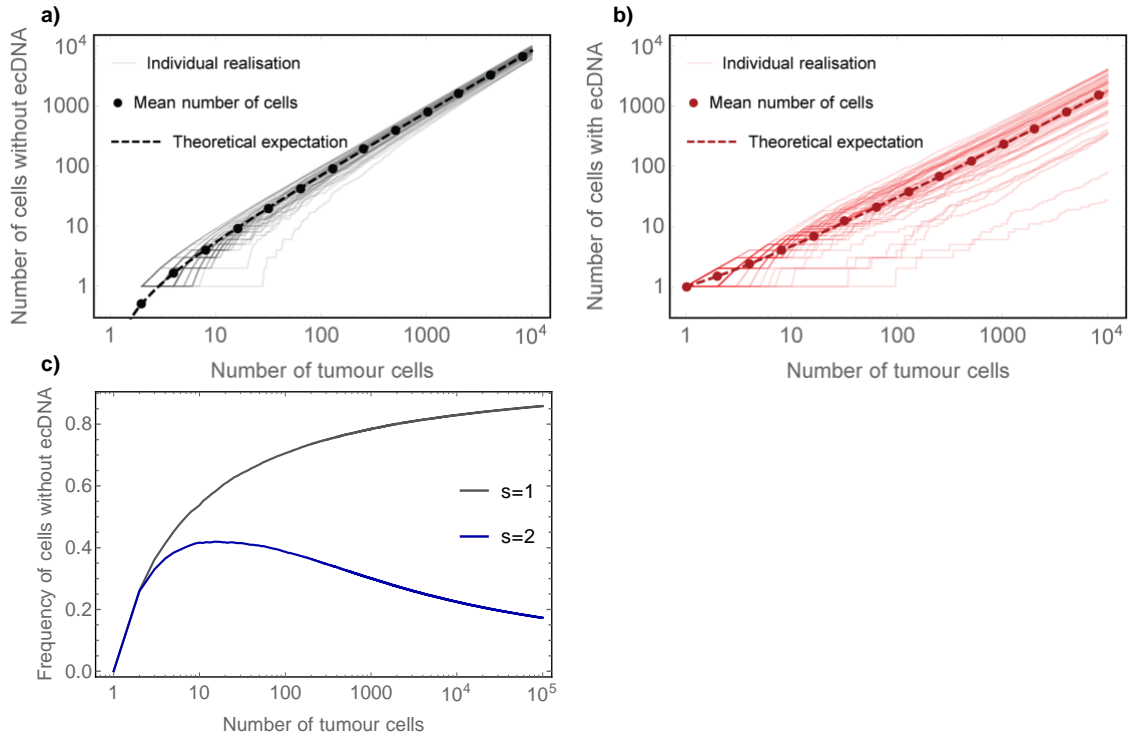
419
 420 Rearranging terms gives

421
 422
$$v(N^+(t)) = 1 - \frac{1}{N^+(t)} \frac{dN^+(t)}{dt}$$

423
 424 and thus we can find for the fraction of cells without ecDNA the following relation

425
 426
$$\frac{1}{1 - f^-(t)} \frac{df^-(t)}{dt} + \frac{1}{N^+(t)} \frac{dN^+(t)}{dt} = 0.$$

427
 428
 429 This equation can be integrated by separation of variables. With the initial condition $N^+(0) =$
 430 1 and $f^-(0) = 0$ the number of cells with ecDNA is given by



431
432

433 **Figure SI 9.** Comparison of average deterministic dynamics of cells a) without and b) with copies of ecDNA for
 434 neutral ecDNA dynamics ($s = 1$). Dots show the average dynamics of neutral stochastic simulations, lines are
 435 individual realisation of the same neutral stochastic process and dashed lines show analytical predictions.
 436 Between tumour variation is considerable, especially for small tumour populations. c) Fraction of cells without
 437 ecDNA over time. In the neutral case $s = 1$ the tumour will be dominated by cells without ecDNA, also the fitness
 438 of cells with and without ecDNA is the same. Under strong positive selection, where cells with ecDNA have a
 439 selection advantage $s = 2$, the frequency of cells without ecDNA approaches 0. Even for strong positive selection
 440 we observe a transient increase of cells without ecDNA.

441
442

$$N^+(t) = (1 - f^-(t))e^t.$$

444

445 Stochastic simulations show that for neutral dynamics, $\frac{N^-(t)}{N^+(t)} = \frac{1}{2}t$ and therefore the fraction
 446 of cells without ecDNA changes according to

447

$$f^-(t) = \frac{N^-(t)}{N^+(t) + N^-(t)} = \frac{1}{\frac{N^+(t)}{N^-(t)} + 1} = \frac{1}{\frac{2}{t} + 1} = \frac{t}{2 + t}.$$

449
450

451 We see that $f^-(0) = 0$ and $f^-(t \rightarrow \infty) \rightarrow 1$, in the long run a growing population with
 452 neutral ecDNA elements will be dominated by cells without ecDNA. This can also be seen from
 453 the fraction of cells carrying ecDNA. From the simple condition $f^-(t) + f^+(t) = 1$ we find

454

$$f^+(t) = 1 - \frac{t}{2 + t} = \frac{2}{2 + t} = \frac{2}{2 + \text{Log}[N]}.$$

455
456

457 Also, the number of cells with ecDNA continuously decreases in the neutral case, the decrease
 458 is proportional to $\sim \text{Log}^{-1}[N]$ and thus relatively slow. For example, in a population of 10^3
 459 cells, the expected fraction would be 22%, in a population of 10^6 cells the fraction becomes
 460 13% and in a population of 10^{11} cells it is 7%. With single cell resolution, we might expect to
 461 detect low levels of neutral ecDNA copies in tumour populations.

462

463 The population dynamics changes when ecDNA is under positive selection. As previously, we
 464 introduce a selection coefficient $s > 0$, with $s = 1$ corresponding to neutral selection and
 465 $s > 1$ to a selective advantage of cells carrying ecDNA. The population level dynamics now
 466 changes to

467

$$\begin{aligned} \frac{dN^-(t)}{dt} &= N^-(t) + sv(N^+(t))N^+(t) \\ \frac{dN^+(t)}{dt} &= sN^+(t) - sv(N^+(t))N^+(t) \end{aligned}$$

470

471 Following the same steps as above, this can be transformed in a single set of equations

472

$$(s - 1)f^-(t) + \frac{1}{1 - f^-(t)} \frac{df^-(t)}{dt} + \frac{1}{N^+(t)} \frac{dN^+(t)}{dt} = s$$

474

475 Again, this equation can be formally integrated by the separation of variables and we get

476

$$N^+(t) = (1 - f^-(t))e^{st - (1-s) \int_0^t f^-(\tau) d\tau}$$

478

479 A closed solution is more challenging in the selection case as we do not have a closed
 480 expression for $\int_0^t f^-(\tau) d\tau$. However, we find numerically $f^-(t \rightarrow \infty) \rightarrow 0$ and thus for
 481 sufficiently long time, the number of cells with ecDNA grows with $N^+(t) \approx e^{st}$. A tumour
 482 population with ecDNA copies under positive selection, will be dominated by cells carrying
 483 ecDNA.

484

485 **4.2 Dynamic predictions of ecDNA under neutral vs positive selection**

486

487 In the previous chapter, we have discussed the stochastic dynamics of the ecDNA copy
 488 number distribution as well as the deterministic aspect of the population dynamics of cells
 489 with and without ecDNA in exponentially growing populations. This leads to three major
 490 predictions that differ between cell populations under neutral dynamics or positive selection.

491

492 (i) Fraction of cells with and without ecDNA: Theory predicts that the fraction of cells
 493 with ecDNA approaches 0 under neutral dynamics and approaches 1 if ecDNA is
 494 under positive selection. The rate of convergence depends on the strength of
 495 selection. In all patient and cell line samples, we find a very high fraction of cells
 496 with ecDNA, suggesting positive selection.

497

498 (ii) Average ecDNA copy number per cell: Theory predicts that the average ecDNA
 499 copy number per cell increases in time, if ecDNA is under positive selection and
 500 remains on average at 1 if ecDNA is under neutral selection. In all patient and cell

501 line samples we find average ecDNA copy numbers $\gg 1$, suggesting positive
502 selection.

503

504 (iii) Power law scaling of the ecDNA copy number distribution: Theory predicts a
505 1/copy number scaling of the ecDNA copy number distribution for both neutral
506 and positive selection. We find this scaling in patient and cell line experiments.
507 However, the ecDNA copy number distribution shifts towards higher copy number
508 under positive selection and consequently, the power law tail is shifted towards
509 higher ecDNA copy number as well. We observe these behaviours in patient and
510 cell line experiments.

511

512

513